RESEARCH ARTICLE

Mesoporous silica chips for selective enrichment and stabilization of low molecular weight proteome

Ali Bouamrani[1], Ye Hu[2]*, Ennio Tasciotti[1]*, Li Li[3], Ciro Chiappini[2], Xuewu Liu[1]** and Mauro Ferrari[1,2,4,5]***

[1] Department of Nanomedicine and BioMedical Engineering, University of Texas Health Science Center at Houston, Houston, TX, USA
[2] Department of Biomedical Engineering, University of Texas at Austin, Austin, TX, USA
[3] Research Center of Protein Chemistry and Proteomic Core Laboratory, Brown Institute of Molecular Medicine, University of Texas Health Science Center at Houston, Houston, TX, USA
[4] Department of Experimental Therapeutics, University of Texas MD Anderson Cancer Center, Houston, TX, USA
[5] Department of Bioengineering, Rice University, Houston, TX, USA

Received: May 24, 2009
Revised: September 19, 2009
Accepted: November 12, 2009

The advanced properties of mesoporous silica have been demonstrated in applications, which include chemical sensing, filtration, catalysis, drug delivery and selective biomolecular uptake. These properties depend on the architectural, physical and chemical properties of the material, which in turn are determined by the processing parameters in evaporation-induced self-assembly. In this study, we introduce a combinatorial approach for the removal of the high molecular weight proteins and for the specific isolation and enrichment of low molecular weight species. This approach is based on mesoporous silica chips able to fractionate, selectively harvest and protect from enzymatic degradation, peptides and proteins present in complex human biological fluids. We present the characterization of the harvesting properties of a wide range of mesoporous chips using a library of peptides and proteins standard and their selectivity on the recovery of serum peptidome. Using MALDI-TOF-MS, we established the correlation between the harvesting specificity and the physicochemical properties of mesoporous silica surfaces. The introduction of this mesoporous material with fine controlled properties will provide a powerful platform for proteomics application offering a rapid and efficient methodology for low molecular weight biomarker discovery.

Keywords:
MS / Nanoproteomics / Nanotechnology / Peptide stabilization / Prefractionation techniques / Surface modification

1 Introduction

The introduction of proteomic tools, especially development in MS [1, 2], has allowed the investigation of complex proteomes and the identification of proteins in cells, tissues and body fluids, increasing the interest of proteomic biomarker research [3, 4]. Many studies suggest that the circulating peptidome is correlated to the pathological status of the patient [4–6]. A critical aspect of the development of MS based proteo- and peptidomics is the broad assortment of molecular species in blood, with concentrations ranging over more than 10 orders of magnitude [7]. This wide dynamic range limits the detection of disease-related peptides present in trace amounts within a large background of abundant and non-relevant proteins. Despite the advances in protein analysis [8, 9], the detection of low

Correspondence: Dr. Mauro Ferrari, Department of Nanomedicine and Biomedical Engineering University of Texas Health Science Center, 1825 Pressler St. Suite 537, Houston, TX 77030, USA
E-mail: mauro.ferrari@uth.tmc.edu
Fax: +1-713-500-2462

Abbreviations: HMS, hexamethyldisilazane; **HMW,** high molecular weight; **LMW,** low molecular weight; **MSC,** mesoporous silica chips; **PPG,** polypropyleneglycol; **SAXS,** small angle X-ray scattering; **TEM,** transmission electron microscopy; **TMB,** 1,3,5-trimethyl benzene

*These authors contributed equally to this work.
**Shared senior authorship.

abundant markers and low molecular weight (LMW) species remains a critical challenge [10–12]. Current strategies to resolve complex proteomes require sample fractionation and depletion prior to MS analysis, limiting throughput and introducing other concerns for experimental variability, reproducibility, sample handling procedures and protein stability during sample processing [13–16]. Innovative technologies addressing these issues are mandatory for biomarkers discovery. The development of nanomaterials, with controllable features offering advantageous new physicochemical properties, has widely improved the use of nanotechnology in biomedical applications. The discovery of mesostructured materials in the 1990s [17, 18] boosted a great deal of research on the preparation [19–23], characterization [24] and morphological control [25, 26] of surfactant-templated mesoporous materials. In previous work, we demonstrated the proof-of principle of LMW molecular uptake in mesoporous particles [27] and surfaces [28, 29]. With tunable pore dimension, pore texture, and surface properties, the mesoporous films are the perfect tools for proteomics applications. In this study, we engineered mesoporous silica chips (MSC) with organized pore structures and a wide range of pore sizes and showed the correlation between the surface properties at the nanoscale and the selectivity in the recovery of proteins and peptides. We further demonstrated the conservation and the long-term stability of proteins and peptides in the porous matrix of the MSC and evaluated the efficiency and reproducibility of this technology for the investigation of complex biological samples.

2 Materials and methods

2.1 Fabrication of mesoporous proteomic chips

The coating solution was prepared by starting with the hydrolyzed silicate precursor solution. First, we added 14 mL of tetraethylorthosilicate into the mixture of 17 mL of ethanol, 6.5 mL of deionized water and 2 mL of 2 M HCl under strong stirring. The silica sol-gels were ready for use after being heated at 75°C for 2 h. The polymer template solutions were prepared by the addition of tri-block copolymer (BASF: L31, L35, L64, L121, P123, F38, F88, F108, F127) in 10 mL of ethanol at room temperature. For the preparation of mesoporous silica films with large pore size, a swelling agent, polypropyleneglycol (PPG) or 1,3,5-trimethyl benzene (TMB) was added in the ethanol solution of polymer before mixing with silicate. The film was obtained by spin-coating the solution on a silicon wafer: 1.5 mL of coating solution was dispensed on a 4'' silicon wafer, and spun at 600 rpm for 5 s followed by 3000 rpm for 30 s. The coated film was aged in an oven at 80°C for 15 h. The oven temperature was raised to 425°C at a rate of 5°C/min. The wafer was kept at 425°C for 4 h, and slowly cooled to room temperature. Oxygen plasma treatment was performed in a Plasma Asher (March Plasma System). Coating of hexamethyldisilazane (HMDS) was performed in a HMDS vapor prime oven (YES) at 150°C for 5 min.

2.2 Characterization

The thickness and porosity of the obtained films were measured with a variable angle spectroscopic ellipsometer (J. A. Woollam Co. M-2000DI). Ellipsometric values, Δ and ψ were measured in the 300–1000 nm range at three incidence angles, 55°, 60°, 65°, respectively, and fitted using the Effective Medium Approximation (EMA) model with WVASE32 software. The surface area and pore size of the mesoporous films were measured using N_2 adsorption–desorption isotherms on a Quantachrome Autosorb-3B Surface Analyzer. Nanopore size distributions were calculated from the adsorption branch of the isotherms using Barrett-Joiner-Halenda model. Contact angles of film surface were measured by a goniometer with captive bubble contact angle measurement.

2.3 Fractionation procedure

We have selected twenty-six peptides and proteins with broad range of molecular weight (900–66 500 Da), p*I* (p*I* 4.0–10.2), and structure. Identity and purity of each peptide and protein was verified by MS and combined, dried by vacuum centrifugation, and stored at −20°C. The molecular weight standards solution was prepared in 135 μL of sterile, deionized water (the final concentration of each standard is presented in the Supporting Information Table 1).

Ten microliters of samples (standards solution or human serum) was spotted onto the mesoporous surface of the MSC. The samples were incubated for 30 min in a wet chamber (100% humidity) to prevent sample evaporation. MSC surface was washed five times with 15 μL of sterile, deionized water. Proteins were eluted from the pores by using 10 μL of a 1:1 mixture of ACN and 0.1% TFA (v/v).

2.4 MS

A matrix solution of 5 mg/mL α-CHCA (Sigma) in a 1:1 mixture of ACN and 0.1% TFA (v/v) and a saturated matrix solution of *trans*-3,5-dimethoxy-4-hydroxycinnamic acid (SA, Sigma) in 2:1 mixture of ACN and 0.1% TFA was used for LMW and high molecular weight (HMW) peptides and proteins, respectively. Each sample was mixed with the appropriate matrix in a 1:3 ratio, and spotted in duplicate onto the MALDI plate. Mass spectra were acquired on a Voyager-DE^{TM}-STR MALDI-TOF (Applied Biosystems, Framingham, MA, USA) mass spectrometer in liner positive-ion mode, using a 337 nm nitrogen laser. Samples were evaluated at two m/z ranges. For the m/z range of

800–10 000 Da, setting were optimized at acceleration voltage 20 KV, grid voltage 19 KV, guide wire voltage 1 KV, delay time 180 ns, and low-mass gate 800. For the m/z range of 3,000–100 000 Da the instrument was optimized at acceleration voltage 25 KV, grid voltage of 23.25 KV, guide wire voltage 6.25 KV, delay time of 500 ns and low mass gate 3000. Each spectrum was the average of 300 laser shots. The spectra were calibrated externally using the ProteoMass standards of peptides and proteins (Sigma) in each mass range.

2.5 Data processing and statistics

The raw spectra were processed with the Voyager Data Explorer software version 4.0 (Applied Biosystems) and the data were exported to SpecAlign [30, 31] software for pretreatment. All spectra were aligned using the PAFFT correlation method and intensity was normalized to TIC. The baseline was corrected and the negative values were removed prior to analysis. Hierarchical clustering was performed using Cluster software and visualized with Treeview software. The MALDI Data (m/z peak intensities) were log-transformed, normalized and median centered. Pearson correlation was used to calculate the distance between the samples, and complete linkage clustering was performed [32]. For supervised hierarchical clustering, an independent Student's t-test was used for comparison between groups ($n = 2$ groups) for each detected MS peak. A p value of 0.02 or lower was considered significant to select differentially harvested peptides and proteins among the different mesoporous proteomic chips (large pores *versus* small pores, hydrophobic *versus* hydrophilic, the swelling agents TMB *versus* PPG).

3 Results and discussion

3.1 Fabrication and characterization of mesoporous proteomic chips

The MSC were produced by the evaporation-induced self-assembly procedure under acidic conditions using Pluronic triblock copolymers as structural templates [33, 34]. The pH of precursor solutions was controlled at 1.5 to prevent the precipitation of mesoporous silicate and balance the procedure between the silicate hydrolysis and condensation of hydrolyzed silicate to polymer micelle. In Fig. 1 are illustrated the schematics of the chemical composition of the coating solution during the production of the mesoporous silica films and the assembly of the final chips (Fig. 1A–D). Manufacturing protocols were optimized to obtain smooth, crack-free surfaces across 4'' silicon wafers as verified by scanning electron microscopy (SEM) and transmission electron microscopy (TEM) imaging of the chip's cross sections (Fig. 1E and F). Porosity was related to the ratio between copolymer and tetraethylorthosilicate, while the thickness was determined by many factors, including the

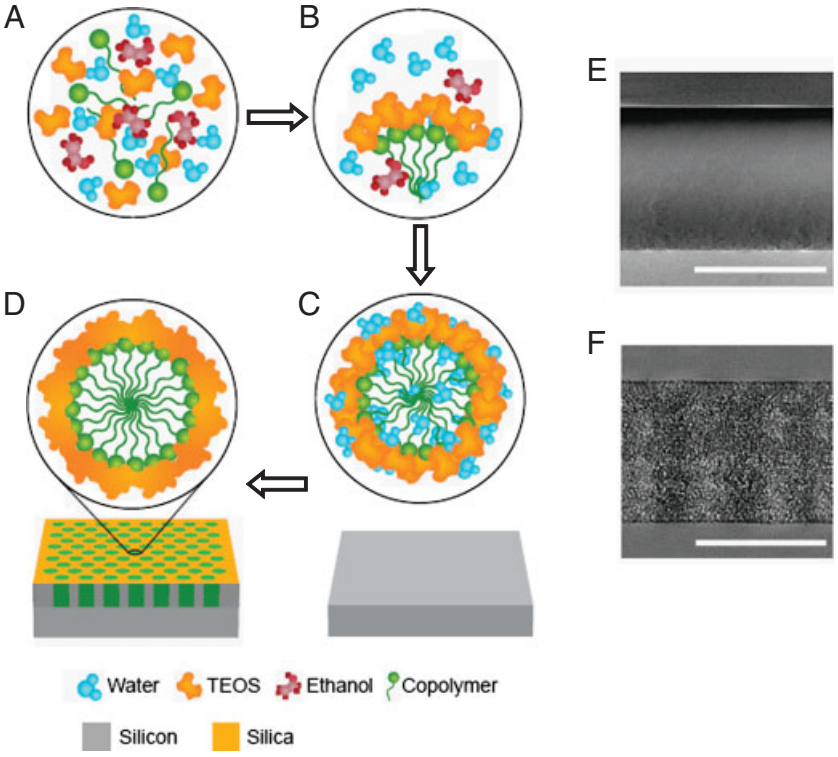

Figure 1. Production and assembly of MSC for proteomic applications. (A–D) Schematic evolution of the chemical composition of the coating solution during the production of a mesoporous silica film. (A) Fresh coating solution; (B) formation of micelles; (C) evaporation-induced self-assembly during spin-coating process; (D) zoomed in view of a pore after aging at elevated temperature; (E) bulk silicon wafer surface; (F) mesoporous silica film on a bulk silicon wafer. (E, F) Cross-section view of GX6 chip by SEM and TEM imaging, respectively (scale bar is 500 nm).

concentration of surfactant, the spin-coating speed, and the aging time of the coating solution. The pore alignment was induced by strain during the spin-coating process [35]. The N_2 adsorption–desorption isotherms of six selected MSC are shown in Fig. 2A. The isotherms can be classified as type-IV curve with H2 hysteresis loops, according to the standard of the International Union of Pure and Applied Chemistry [36]. This type of hysteresis indicated ink-bottle shaped pores, and non-ordered worm-like pore arrangement. For this type of isotherm, adsorption branch of the isotherm can be used to calculate the pore size distribution. The pore size distribution curves (values ranging from 2.7 to 9 nm) were derived from adsorption isotherms using Barrett-Joyner-Halenda method (Fig. 2A, right panel).

The reflection small angle X-ray scattering (SAXS) curves of the films are shown in Fig. 2B. The curves were recorded 2 cm off the center of the 4'' wafer, with the beam incidence along the direction of radius. The SAXS curve showed a peak around 0.5°–0.7° (corresponding to d-space around 13–17 nm), suggesting a periodic order in the spatial variation of the electron density in the film, and some degree of alignment of the pores. This was further confirmed by atomic force microscopy (AFM) measurement of the film surface (Fig. 2C). The image showed different dimensions of the features along and perpendicular to the radius.

Different chemical modifications were also studied. Oxygen plasma treatment was applied to ensure the hydrophilicity, while HMDS coating was applied to make the surface hydrophobic. The hydrophilicity of the films was evaluated through contact angle measurement. The O_2 plasma treated films showed $<15°$ contact angle, while the HMDS coated film showed $>65°$ contact angle (see Supporting Information Table 2 and Fig. 1 for detailed properties of the different mesoporous surfaces and TEM images).

3.2 Enrichment of the LMW proteome

High-throughput MS is a gold standard for protein expression profiling and for disease-related biomarker discovery [1]. However, the current MS technologies are not able to profile the entire proteome and particularly the LMW species because of the interfering signals generated by the highly abundant, HMW proteins [9]. To address this limitation, we developed a fractionation method using the MSC to efficiently and specifically enrich the LMW proteome from complex biological samples. The principle of this fast on-chip fractionation strategy is shown in Fig. 3A: (i) the sample is spotted on the chip surface and LMW molecules are trapped into the pores during the incubation

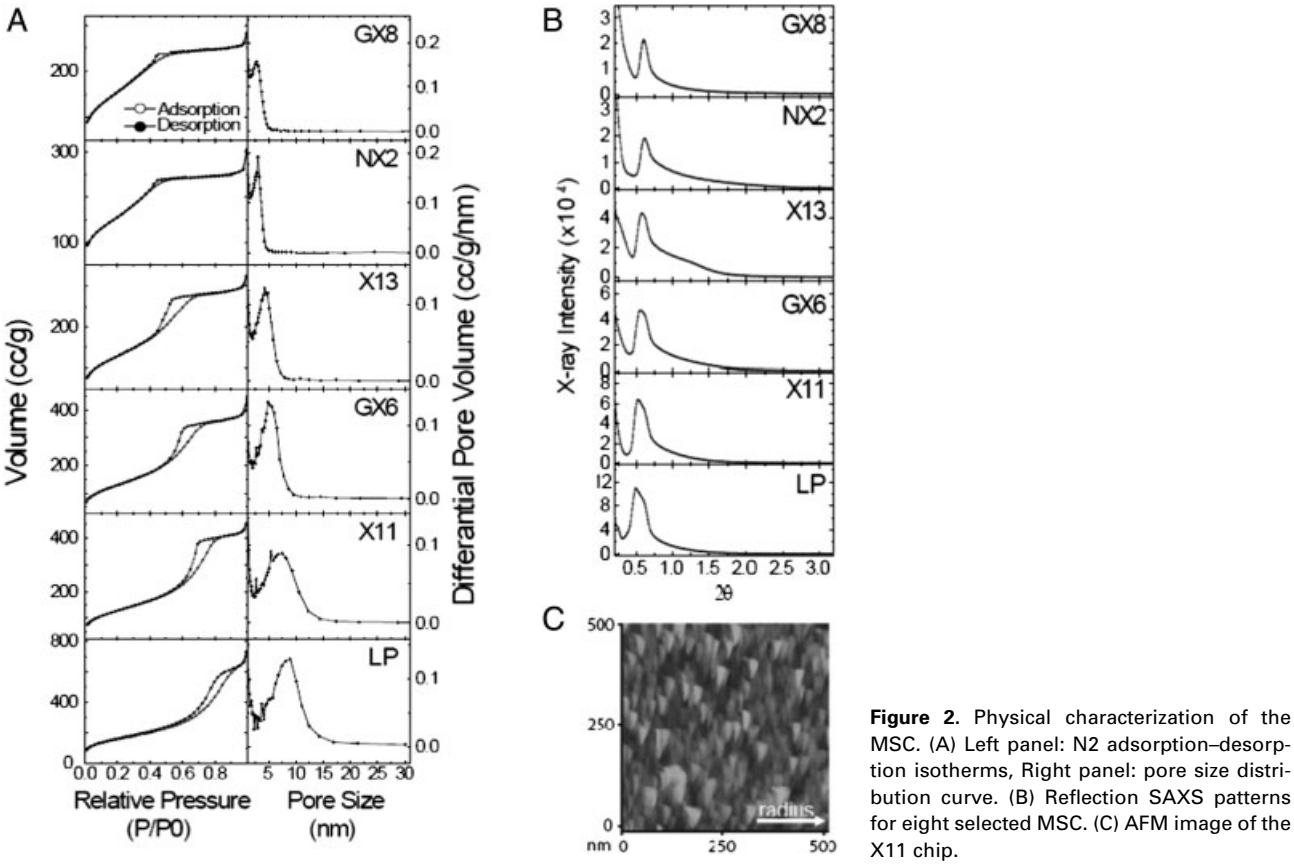

Figure 2. Physical characterization of the MSC. (A) Left panel: N2 adsorption–desorption isotherms, Right panel: pore size distribution curve. (B) Reflection SAXS patterns for eight selected MSC. (C) AFM image of the X11 chip.

step; (ii) the larger protein species remain outside the pores and are removed during the washing steps; (iii) the enriched small molecules are then eluted from the pores and further analyzed by MS. To evaluate the fractionation and enrichment efficacy of this on-chip strategy, and to characterize how the physicochemical properties of the chips correlate with their harvesting properties, we have selected 26 standard peptides and proteins with a broad range of molecular weights (900–66 500 Da) and p*I*s (p*I* 4.0–10.2), and we have combined them to represent the diversity and complexity of biological samples (See Supporting information Fig. 2 and Table 1). Figure 3B and C show the high detection signals of the standards when separated into two different solutions for the peptide range (16 markers from 900 to 8500 Da) and the protein range (16 markers from 3400 to 66 500 Da). When combined in a unique solution, the detection signal in the peptide range dramatically decreased while the larger proteins remained well detected (Fig. 3D and E). The MS detection signal suppression in the LMW observed with the combined solution of molecular markers mimics the results obtained with MS analysis of complex body fluids such as serum and plasma. The presence of higher amount of HMW molecules such as Albumin and other large proteins impede the detection of the LMW species. The results presented in Fig. 3F and G demonstrate the ability to eliminate the big proteins and to increase significantly the detection of the LMW peptides and proteins.

The capacity of MS approaches to investigate low abundant proteins in biological samples composed of highly complex proteomes such as serum body fluids is a major issue for the detection of potential biomarkers [2, 3, 10]. To assess the limit of detection of our technology, human serum sample was spiked with a known peptide (Neurotensin, 1673 Da) at different concentration levels before MSC fractionation and MALDI analysis. The results presented in Fig. 4 demonstrated the ability of the method to identify the spiked neurotensin in a concentration as low as 2 ng/mL.

3.3 Pore size selectivity of the LMW enrichment

To assess the size-dependant depletion of HMW proteins, we have developed 6 proteomic chips with pore sizes ranged from 2.0 to 11.7 nm. A variety of pore sizes was first obtained by using different polymer templates with different volume ratio of hydrophilic/hydrophobic composition. Because of its highest hydrophobic/hydrophilic ratio among pluronic surfactants, L121 is capable of forming the mesoporous silica with the largest porosity (~55%) and pore size

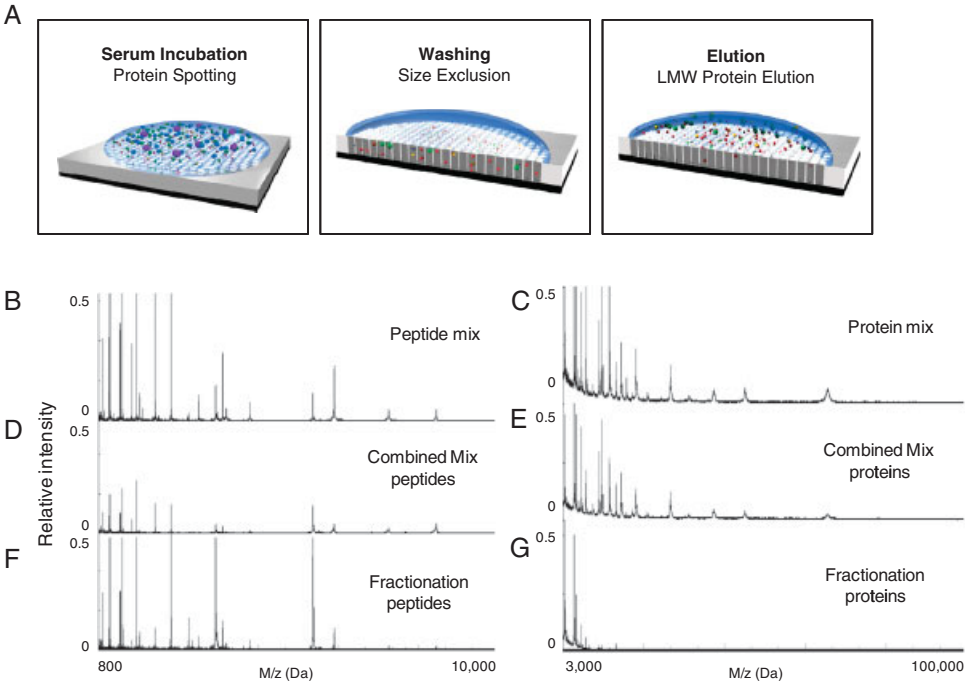

Figure 3. Principle of MSC fractionation and LMW enrichment. (A) After sample spotting on the surface, LMW proteins and peptides are trapped into the pores while the larger species remained outside the pores and are removed during the washing steps. The enriched fractions are then eluted and analyzed by MALDI. (B, C) Detection of the molecular weight standards by MALDI-TOF in the peptide range (800–10 000 Da) and in the protein range (3000–100 000 Da). For the separated mixes of peptides (16 markers from 900 to 8500 Da) and proteins (16 markers from 3400 to 66 500 Da), the profiles present a high level of detection for each species. (D, E) In the combined mix, the signal suppression of LMW standards is due to the high concentration of HMW proteins. (F, G) In the MALDI profiles of the combined standard mix after fractionation on the MSC, the detection of LMW markers is significantly increased compared to the unprocessed sample.

(5.2 nm). In addition, by applying a different ratio of swelling agent such as PPG to the L121 pluronic surfactant, the pore size has been further enlarged to obtain MSC with 7.4, 9.0 and 11.7 nm. To evaluate the molecular cut-off and the enrichment properties of the different pore sizes, we fractionated the solution of peptide and protein standards on the set of MSC ranging from 2.0 to 11.7 nm. The removal of the large proteins is size dependant as illustrated by the gradual decrease of the molecular cut-off observed for the different chips (Fig. 5A). The silica surface with 9.0 nm pores did not completely exclude albumin, according to its three-dimensional structure which exhibits an average size of 8 by 3 nm [37]. This analysis demonstrates the size exclusion principle of the mesoporous chip fractionation, and reveals the limit of this depletion approach observed with the 11.7 nm pores which provides a similar MS pattern to the non-fractionated sample (Fig. 5B).

In addition to the size-dependant depletion of HMW proteins, the on-chip fractionation of the standards solution displays a differential and selective enrichment of LMW species associated with the pore sizes. The two-way hierarchical clustering presented in Fig. 5C shows the LMW standards enrichment pattern obtained with the different MSC. Even if all the peptides are below the molecular cut-off of the chips, there is a positive correlation between the pore sizes and the molecular weight of the trapped species. The MSC with large pores, up to 9 nm, preferentially harvest bigger peptides, while smaller peptides are recovered more efficiently by the chips with smaller pores. The chips with 11.7 nm pores present no significant improvement

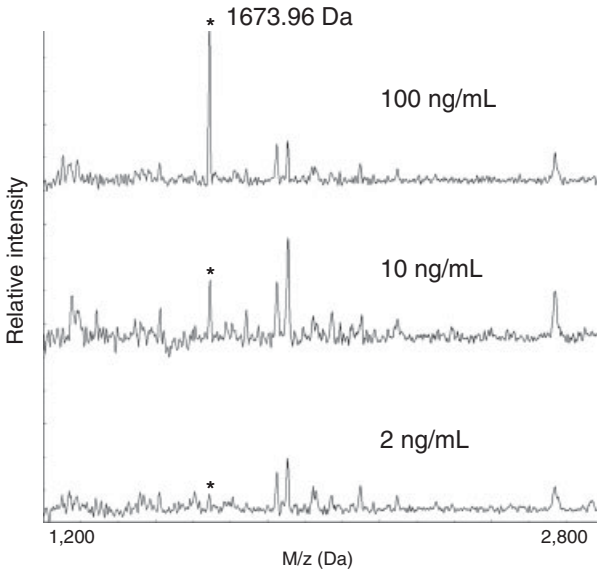

Figure 4. Sensitivity of the MSC enrichment. Mass spectra of spiked human serum sample with decreasing concentrations of neurotensin peptide (1673.96 Da): 100, 10 and 2 ng/mL (from top to bottom).

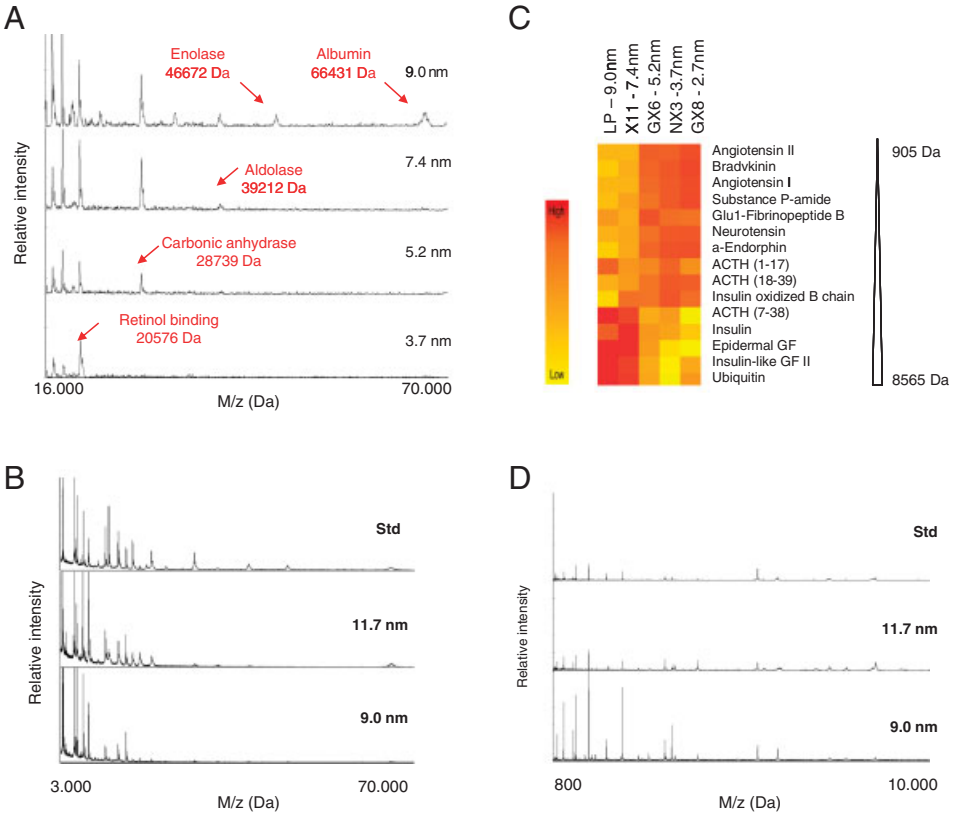

Figure 5. Molecular cut-off and size-dependent enrichment of the MSC. (A) Magnified view of the MALDI spectra demonstrating the characteristic molecular cut-off of each MSC correlating to the pore size. (B) MALDI profiles of the HMW region for the standards solution before (Std) and after fractionation on 11.7- and 9.0-nm pores MSC. (C) Two-way hierarchical clustering of the peptide mix features among the different chips. The intensity of the red or yellow color indicates the relative peptide concentration. Larger pores enhanced the harvesting of bigger peptides (from 3600 to 8500 Da), while the small peptides (from 900 to 3500 Da) were preferentially recovered from the chips with smaller pores. (D) MALDI profiles of the LMW region for the standards solution before (Std) and after fractionation on 11.7 and 9.0 nm pores MSC.

in the LMW region detection (Fig. 5D). This result indicates the size limit of the MSC for an efficient enrichment strategy.

3.4 Identification of the selective fractionation patterns due to MSC's nanofeatures

In the analysis of the fractionation and enrichment of LMW species from human serum, we subdivided the chips in three categories according to (i) pore size, (ii) wettability, and (iii) pore geometry and surface morphology. We performed unsupervised two-way hierarchical clustering (2-D complete linkage) to analyze the overall MALDI profiles of the different MSC. (Fig. 6A). Depending on their harvesting characteristics, selective nanopore size and specific recovery patterns, each of the MSC consistently identified unique proteomic signatures, as shown in the supervised hierarchical clustering (Fig. 6B–D). Using a multi-chip strategy and combining the MS profiles obtained from five different MSC we obtained a threefold increase in the number of detected peptides and proteins in the LMW range with respect to plain unprocessed serum (Fig. 6E and F and Supporting Information Fig. 5). These results showed that the different nanofeatures (structure, size and chemistry of the pores) on the MSC conveyed different functionalities and served as analytical "first order processors" of this technology. According to this strategy, a multitude of chips can be used simultaneously to increase the amount of information recovered from the serum.

3.5 Sample stability and reproducibility of the harvesting procedure

Reproducibility and reliability are crucial factors for any assay to be used in the clinical setting. Several publications reported that pre-analytical sample management might lead to significant alterations of the proteomic profiles and the generation of artifacts [13, 16]. We assessed the consistency of our on-chip fractionation assay reproducing the same experiment in six replicates. After fractionation, the spectra of the replicates showed highly reproducible MS signals (Supporting

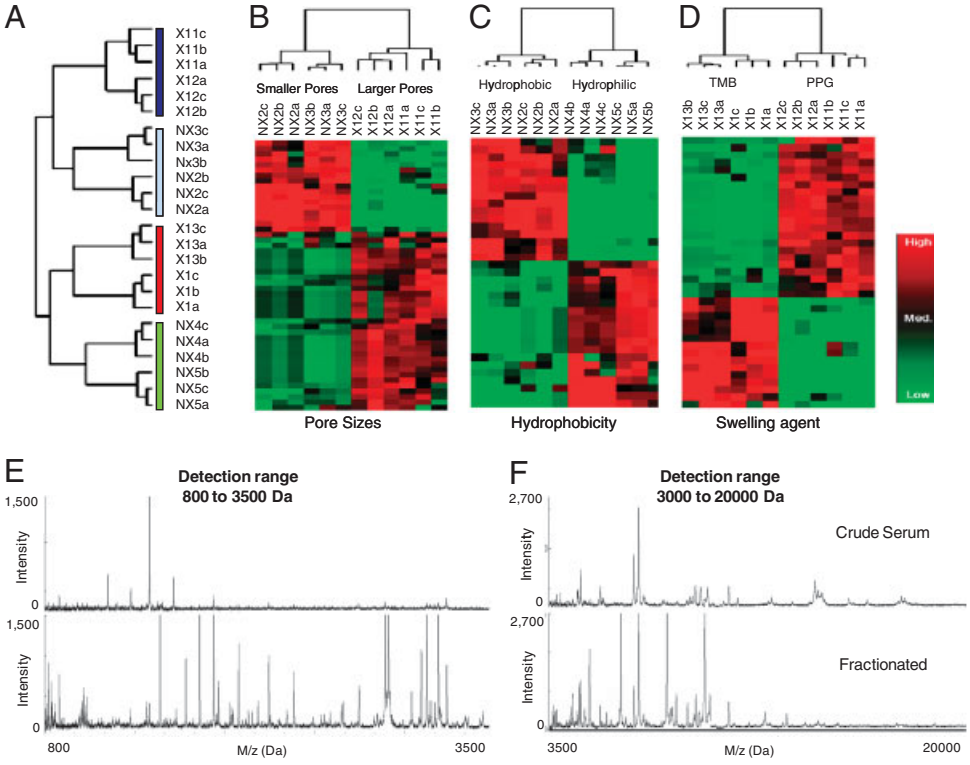

Figure 6. Effect of pore sizes and chemical properties on serum peptide harvesting. (A), Dendogram of the unsupervised two-way hierarchical clustering. Each set of MSC is uniquely identified. The dark and light blue rectangles represent large and small pores, respectively. The green and red rectangles represent the hydrophobic and TMB-generated MSC, respectively. (B–D) Supervised hierarchical clustering and specific recovery pattern for each set of MSC as indicated in the figure. The relative intensity is gradually indicated with red squares (high intensity), black squares (median) and green squares (low intensity or absence of a peak). The entire hierarchical clusters are presented in Supporting Information Figs. 3 and 4. (E, F) The MS profiles obtained from crude serum (E) or from purified peptides and proteins using the multi-chip strategy (F). The multi-chip profile was obtained by combining the spectrum from each MSC-purified fraction.

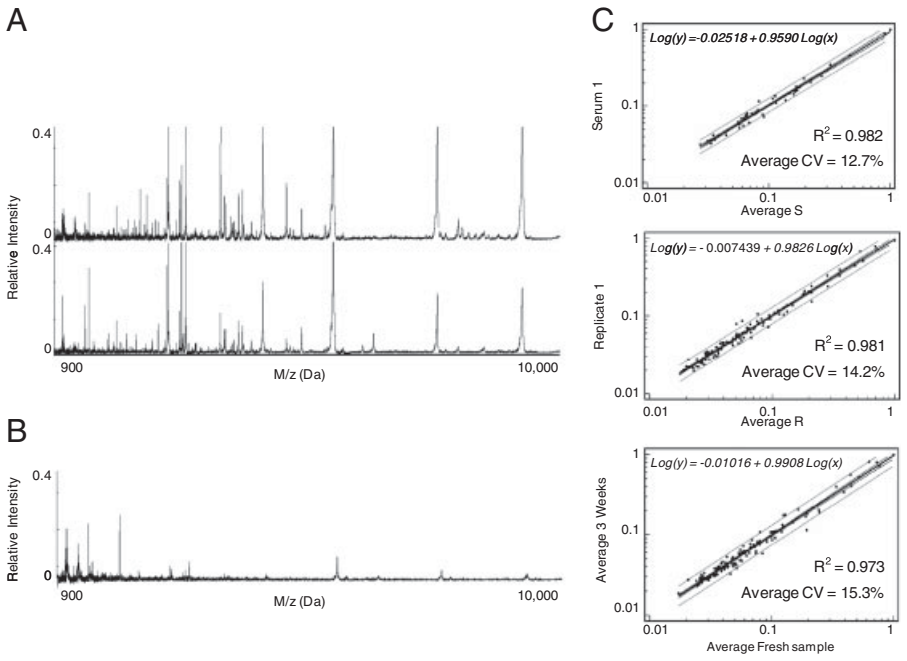

Figure 7. On-chip stabilization of fractionated serum. (A) Representative MALDI profiles of LMW peptides and proteins eluted immediately after serum fractionation or after 3 wk of on-chip storage at room temperature. (B) MS spectrum of LMW fraction of serum sample dried and stored on nonporous silicon surface. (C) From top to bottom: Linear regression analysis of average intensities of detected MS peaks in each replicate compared to replicate 1 for crude serum, freshly fractionated serum and fractionated serum after 3 wk MSC storage at room temperature. Equation, CV and coefficient of determination (R^2) are indicated.

Information Fig. 6). To evaluate protein stability, the MSC were incubated with human serum, dried after washing, and stored for 3 wk at room temperature. The protein/peptide patterns obtained were comparable with those of freshly fractionated serum (Fig. 7A), as confirmed by the results of the statistical analysis showed in Fig. 7C. The variability of the peak signals measured by the average CV was estimated at 12.7% for crude serum and at 14.2% for the fractionated samples. The marginal variations could be due to the internal variability of the MALDI instrument and suggested that the on-chip pretreatment and storage did not induce any significant alteration of the MS protein profiles. The same experiment has been performed on non porous silicon. The dried serum recovered after storage on silicon surface was fractionated on the MSC before MALDI analysis. The poor MS profile obtained demonstrated the stabilization advantage of the mesoporous surface. In analogy with previously postulated mechanisms, we hypothesize that the LMW species trapped inside the nanopores were preserved from degradation through the size exclusion of proteases, or by steric inhibition of their proteolytic activity in the confined space of the nanopores [38, 39].

The establishment of a simple sample acquisition and storage protocol, and the ability to impede further degradation of the proteins and peptides once they are captured, are essential for translation into the laboratory clinical practice [40, 41]. With prior methodologies, deceptive results confounded the analysis and rendered meaningless the use of the profiles to derive any significant diagnostic or clinical information [10, 11, 41]. On the contrary, after processing on the MSC, the resulting protein patterns were reproducible and consistent even after long term on-chip storage at room temperature.

4 Concluding remarks

Using surfactant-templated mesoporous silica thin films, we have developed a size-exclusion method for a rapid and specific isolation and analysis of LMW peptides from complex biological samples. In combination with MS profiling, we have demonstrated significant improvement and optimization of the specific harvesting efficacy of the MSC. Besides the HMW proteins depletion, we established the correlation between the harvesting capacity and the physicochemical properties of mesoporous silica surfaces. The structural design and the chemical functionalization of the porous silica surface further increase the specificity of peptides enrichment. The wealth of finely tunable and controlled properties on mesoporous silica surfaces could be used for MS-based peptide and protein profiling of complex biological fluids providing a powerful tool in the selective separation and concentration of the LMW proteome.

The MSC are inexpensive to manufacture, and allow for scaled up production to attain the simultaneous processing of a large number of samples, providing advantageous features for exploratory screening and biomarker discovery. They may further be used to store, protect and stabilize biological fluids, enabling the simplified and cost-effective collection and transportation of clinical samples.

The authors thank Professor Rowen Chang and the Research Center of Protein Chemistry Core Laboratory at the university of Texas health science center at Houston for the use of the Mass Spectrometry facility, M. Landry for excellent graphical support, and Y. Flores, Jimenez, M. Way and K. Dara for laboratory assistance. We thank the Microelectronics Research Center, the

Texas Materials Institute and the Center for Nanomaterials, at the University of Texas at Austin, for the use of materials fabrication and characterization facilities. We thank Dr. Elizabeth Donnachie, Research Associate in the Gulf States Hemophilia and Thrombophilia Center at UTHSC-Houston, for providing the serum used in the study. These studies were supported by the following grants: State of Texas's Emerging Technology Fund, NIH (R21/R33CA122864), NASA (NNJ06HE06A), NIH (R01CA128797), DoD CDMRP Breast Cancer Research Program Innovator Award (W81XWH-08-BCRP-INNOV). The authors would like to recognize the contributions and support from the Alliance for NanoHealth (ANH).

The authors have declared no conflict of interest..

5 References

[1] Aebersold, R., Mann, M., Mass spectrometry-based proteomics. *Nature* 2003, *422*, 198–207.

[2] Hanash, S. M., Pitteri, S. J., Faca, V. M., Mining the plasma proteome for cancer biomarkers. *Nature* 2008, *452*, 571–579.

[3] Kulasingam, V., Diamandis, E. P., Strategies for discovering novel cancer biomarkers through utilization of emerging technologies. *Nat. Clin. Pract. Oncol.* 2008, *5*, 588–599.

[4] Liotta, L. A., Ferrari, M., Petricoin, E., Clinical proteomics: written in blood. *Nature* 2003, *425*, 905.

[5] Villanueva, J., Shaffer, D. R., Philip, J., Chaparro, C. A. *et al.*, Differential exoprotease activities confer tumor-specific serum peptidome patterns. *J. Clin. Invest.* 2006, *116*, 271–284.

[6] Petricoin, E. F., Belluco, C., Araujo, R. P., Liotta, L. A., The blood peptidome: a higher dimension of information content for cancer biomarker discovery. *Nat. Rev. Cancer* 2006, *6*, 961–967.

[7] Anderson, N. L., Anderson, N. G., The human plasma proteome: history, character, and diagnostic prospects. *Mol. Cell. Proteomics* 2002, *1*, 845–867.

[8] Shores, K. S., Knapp, D. R., Assessment approach for evaluating high abundance protein depletion methods for cerebrospinal fluid (CSF) proteomic analysis. *J. Proteome Res.* 2007, *6*, 3739–3751.

[9] Tirumalai, R. S., Chan, K. C., Prieto, D. A., Issaq, H. J. *et al.*, Characterization of the low molecular weight human serum proteome. *Mol. Cell. Proteomics* 2003, *2*, 1096–1103.

[10] Diamandis, E. P., Mass spectrometry as a diagnostic and a cancer biomarker discovery tool: opportunities and potential limitations. *Mol. Cell. Proteomics* 2004, *3*, 367–378.

[11] Petricoin, E. F., Ardekani, A. M., Hitt, B. A., Levine, P. J. *et al.*, Use of proteomic patterns in serum to identify ovarian cancer. *Lancet* 2002, *359*, 572–577.

[12] Villanueva, J., Philip, J., Chaparro, C. A., Li, Y. *et al.*, Correcting common errors in identifying cancer-specific serum peptide signatures. *J. Proteome Res.* 2005, *4*, 1060–1072.

[13] Findeisen, P., Sismanidis, D., Riedl, M., Costina, V., Neumaier, M., Preanalytical impact of sample handling on proteome profiling experiments with matrix-assisted laser desorption/ionization time-of-flight mass spectrometry. *Clin. Chem.* 2005, *51*, 2409–2411.

[14] Georgiou, H. M., Rice, G. E., Baker, M. S., Proteomic analysis of human plasma: failure of centrifugal ultrafiltration to remove albumin and other high molecular weight proteins. *Proteomics* 2001, *1*, 1503–1506.

[15] Rabilloud, T., Two-dimensional gel electrophoresis in proteomics: old, old fashioned, but it still climbs up the mountains. *Proteomics* 2002, *2*, 3–10.

[16] Seam, N., Gonzales, D. A., Kern, S. J., Hortin, G. L. *et al.*, Quality control of serum albumin depletion for proteomic analysis. *Clin. Chem.* 2007, *53*, 1915–1920.

[17] Beck, J. S., Vartuli, J. C., Roth, W. J., Leonowicz, M. E. *et al.*, A new family of mesoporous molecular-sieves prepared with liquid-crystal templates. *J. Am. Chem. Soc.* 1992, *114*, 10834–10843.

[18] Kresge, C. T., Leonowicz, M. E., Roth, W. J., Vartuli, J. C., Beck, J. S., Ordered mesoporous molecular-sieves synthesized by a liquid-crystal template mechanism. *Nature* 1992, *359*, 710–712.

[19] Attard, G. S., Glyde, J. C., Goltner, C. G., Liquid-crystalline phases as templates for the synthesis of mesoporous silica. *Nature* 1995, *378*, 366–368.

[20] Huo, Q. S., Margolese, D. I., Ciesla, U., Feng, P. Y. *et al.*, Generalized synthesis of periodic surfactant inorganic composite-materials. *Nature* 1994, *368*, 317–321.

[21] Miyata, H., Kuroda, K., Preferred alignment of mesochannels in a mesoporous silica film grown on a silicon (110) surface. *J. Am. Chem. Soc.* 1999, *121*, 7618–7624.

[22] Yang, P., Deng, T., Zhao, D., Feng, P. *et al.*, Hierarchically ordered oxides. *Science* 1998, *282*, 2244–2246.

[23] Zhao, D. Y., Feng, J. L., Huo, Q. S., Melosh, N. *et al.*, Triblock copolymer syntheses of mesoporous silica with periodic 50 to 300 angstrom pores. *Science* 1998, *279*, 548–552.

[24] Sakamoto, Y., Kaneda, M., Terasaki, O., Zhao, D. Y. *et al.*, Direct imaging of the pores and cages of three-dimensional mesoporous materials. *Nature* 2000, *408*, 449–453.

[25] Wang, J. F., Zhang, J. P., Asoo, B. Y., Stucky, G. D., Structure-selective synthesis of mesostructured/mesoporous silica nanofibers. *J. Am. Chem. Soc.* 2003, *125*, 13966–13967.

[26] Yamaguchi, A., Uejo, F., Yoda, T., Uchida, T. *et al.*, Self-assembly of a silica-surfactant nanocomposite in a porous alumina membrane. *Nat. Mater.* 2004, *3*, 337–341.

[27] Terracciano, R., Gaspari, M., Testa, F., Pasqua, L. *et al.*, Selective binding and enrichment for low-molecular weight biomarker molecules in human plasma after exposure to nanoporous silica particles. *Proteomics* 2006, *6*, 3243–3250.

[28] Gaspari, M., Cheng, M. M. C., Terracciano, R., Liu, X. W. *et al.*, Nanoporous surfaces as harvesting agents for mass spectrometric analysis of peptides in human plasma. *J. Proteome Res.* 2006, *5*, 1261–1266.

[29] Geho, D., Cheng, M. M., Killian, K., Lowenthal, M. *et al.*, Fractionation of serum components using nanoporous substrates. *Bioconjug. Chem.* 2006, *17*, 654–661.

[30] Wong, J. W., Cagney, G., Cartwright, H. M., SpecAlign-processing and alignment of mass spectra datasets. *Bioinformatics* 2005, *21*, 2088–2090.

[31] Wong, J. W., Durante, C., Cartwright, H. M., Application of fast Fourier transform cross-correlation for the alignment of large chromatographic and spectral datasets. *Anal. Chem.* 2005, *77*, 5655–5661.

[32] Eisen, M. B., Spellman, P. T., Brown, P. O., Botstein, D., Cluster analysis and display of genome-wide expression patterns. *Proc. Natl. Acad. Sci. USA* 1998, *95*, 14863–14868.

[33] Lu, Y., Ganguli, R., Drewien, C. A., Anderson, M. T. *et al.*, Continuous formation of supported cubic and hexagonal mesoporous films by sol-gel dip-coating. *Nature* 1997, *389*, 364–368.

[34] Yang, H., Coombs, N., Sokolov, I., Ozin, G. A., Free-standing and oriented mesoporous silica films grown at the air-water interface. *Nature* 1996, *381*, 589–592.

[35] Rice, R. L., Kidd, P., Holmes, J. D., Morris, M. A., Structural comparison of hexagonally ordered mesoporous thin films developed by dip- and spin-coating using X-ray reflectometry and other quantitative X-ray techniques. *J. Mater. Chem.* 2005, *15*, 4032–4040.

[36] Sing, K. S. W., Everett, D. H., Haul, R. A. W., Moscou, L. *et al.*, Reporting physisorption data for gas solid systems with special reference to the determination of surface-area and porosity (Recommendations 1984). *Pure Appl. Chem.* 1985, *57*, 603–619.

[37] He, X. M., Carter, D. C., Atomic structure and chemistry of human serum albumin. *Nature* 1992, *358*, 209–215.

[38] Luchini, A., Geho, D. H., Bishop, B., Tran, D. *et al.*, Smart hydrogel particles: biomarker harvesting: one-step affinity purification, size exclusion, and protection against degradation. *Nano Lett.* 2008, *8*, 350–361.

[39] Vaitheeswaran, S., Thirumalai, D., Interactions between amino acid side chains in cylindrical hydrophobic nanopores with applications to peptide stability. *Proc. Natl. Acad. Sci.* 2008, *105*, 17636–17641.

[40] Banks, R. E., Stanley, A. J., Cairns, D. A., Barrett, J. H. *et al.*, Influences of blood sample processing on low-molecular-weight proteome identified by surface-enhanced laser desorption/ionization mass spectrometry. *Clin. Chem.* 2005, *51*, 1637–1649.

[41] Ransohoff, D. F., Lessons from controversy: ovarian cancer screening and serum proteomics. *J. Natl. Cancer Inst.* 2005, *97*, 315–319.

